10

Regge pole beyond perturbation theory

We address now the most interesting question, namely how much of what we have found in the perturbation theory will survive in the real world where the hadrons interact strongly.

The hadrons and hadron resonances lie on Regge trajectories $\alpha(t)$ which relate the hadron spin σ and the mass, $\sigma = \alpha(m_h^2)$. These trajectories determine the asymptotic behaviour of the scattering in the crossing channel, $t < 0$, where the corresponding quantum numbers can be exchanged.

At the first sight, we succeeded in reggeizing the amplitude and obtained the Regge pole as expected. Unfortunately, the trajectory that we found in the perturbative $g\varphi^3$ theory,

$$\alpha(q^2) = -1 + \bar{g}^2 \int \frac{d^2\mathbf{k}_\perp}{2(2\pi)^3} \frac{m^2}{[m^2 + \mathbf{k}_\perp^2][m^2 + (\mathbf{k}-\mathbf{q})_\perp^2]}\,; \quad (10.1)$$

$$t = -\mathbf{q}_\perp^2; \quad \bar{g}^2 = \frac{g^2}{m^2}\,,$$

does not possess a single particle; as long as the coupling is small, $\bar{g} \ll 1$, the trajectory stays below $j = 0$ at any t (at large $|t|$ it falls like $\ln t/t$). In principle we could get a bound state on the trajectory, or even enforce $\alpha(0) = 1$, if we took a large coupling, $\bar{g}^2 = \mathcal{O}(1)$.

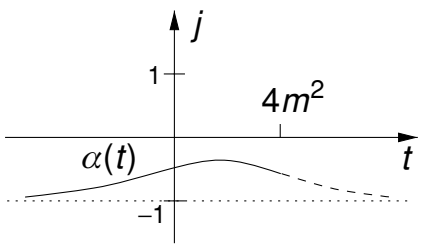

But this means moving outside the boundaries of perturbation theory where we are helpless. The selection of diagrams based on the leading log approximation is here not valid, since all sorts of corrections to the ladder become essential.

https://doi.org/10.1017/9781009290227.011 Published online by Cambridge University Press

If we can hope at all that the realistic hadron Regge-pole picture will be established, then only if the interaction is non-perturbative. In spite of the impossibility to *calculate* the hadron trajectories, we will nevertheless be able to describe the structure of *inelastic processes* that constitute the base of the real Regge poles. And our experience with the investigation of the reggeons in perturbation theory will help us to do that.

10.1 Basic features of multiparticle production

10.1.1 Particle density

The underlying inelastic processes in perturbation theory were dominated by multiperipheral ladders. The simple reason for the ladder dominance was *large invariant pair energies* of the neighbouring particles (see Section 9.2):

$$\langle s_{i,i+1}\rangle = (k_i + k_{i+1})^2 \simeq \beta_i \alpha_{i+1} s \sim \frac{\beta_i}{\beta_{i+1}} m^2_{i+1,\perp} \sim \frac{\beta_i}{\beta_{i+1}} m \gg m^2 \ . \quad (10.2)$$

Particles were distributed scarcely in rapidity (see Section 9.3):

$$\Delta\eta = \langle \eta_i - \eta_{i+1}\rangle \simeq \ln \frac{\langle s_{i,i+1}\rangle}{m^2} \simeq \frac{1}{\beta(0)} \gg 1, \quad (10.3)$$

and the permutation of two particles with large $\Delta\eta$ in (9.29) produced a significant recoil causing high virtuality of the propagator and the suppression of the amplitudes with crossed lines.

With the growth of $\bar{g}^2$ the decays become more frequent, the particle density increases and the pair energies $\langle s_{i,i+1}\rangle$ decrease. The time ordering of successive decays starts to disappear and processes with particle permutations cease to play the rôle of small corrections when we reach $\langle s_{i,i+1}\rangle \sim m^2$ at $\bar{g}^2 \sim 1$.

The key question is whether the particle density will continue to grow with the increase of the interaction strength, or will it stop and freeze at a certain value? Will the rapidity distribution remain homogeneous and independent of the total energy?

The problem we are dealing with reminds that of the one-dimensional gas. We plant a few points into an interval. If there is no repulsion between them, one can stuff in as many points as one wants. If there is, some mean density will be established, depending on the dynamics.

Two statements can be made.

https://doi.org/10.1017/9781009290227.011 Published online by Cambridge University Press

(1) *If the asymptotic behaviour is determined by the Regge pole*, then in multi-particle production processes a certain constant rapidity density of final particles is reached.

(2) *Irrespectively of the Regge pole hypothesis*, a serious reason for arriving at a constant density lies in the astonishing, well established experimental fact that transverse momenta do not grow with energy (at least for energies up to 10^{13} eV).

The first statement can be rigourously proven. The second one is more intuitive but rather general too. Let us start from the latter.

10.1.2 Limited transverse momenta and rapidity plateau

In inelastic high energy hadron interactions particles are produced in two bunches following the directions of the colliding hadrons. If you measure the average transverse momentum of produced particles at different collision energies, you will get

$$\left\langle \mathbf{k}_\perp^2 \right\rangle \;=\; \mathrm{const}(s). \tag{10.4}$$

This is just what happens in the perturbative model that we have used above. There the inclusive cross section decreased rapidly at large $k_\perp$,

$\phi(\mathbf{k}_\perp^2) =$ 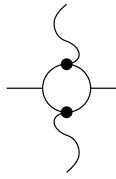 $\sim \int \dfrac{d^2\mathbf{q}_\perp}{(\mathbf{q}_\perp^2)^4} \sim \dfrac{1}{\mathbf{k}_\perp^6}, \qquad \mathbf{k}_\perp^2 \gg m^2,$ (10.5a)

so that the average transverse momentum was of the order of the mass,

$$\frac{\int d^2\mathbf{k}_\perp\, \phi(\mathbf{k}_\perp^2)\cdot \mathbf{k}_\perp^2}{\int d^2\mathbf{k}_\perp\, \phi(\mathbf{k}_\perp^2)} \;=\; \mathrm{const}\cdot m^2. \tag{10.5b}$$

This is a unique feature of the $g\varphi^3$ theory which is too simplistic and specific to have any relation to the real world.

However, as we have already stated, if e.g. fermions are included in the scheme, the integral (10.5b) defining $\left\langle \mathbf{k}_\perp^2 \right\rangle$ becomes *logarithmically divergent*, and the transverse momenta increase with s. In fact, this happens in *any* renormalizable quantum field theory (with the only exception of the *superconvergent* $g\varphi^3$)! Thus it is the experimental situation alone that forces us to look for a theoretical description that would respect (10.4).

Let us show now that if we want $\left\langle \mathbf{k}_\perp^2 \right\rangle$ to be restricted, a finite particle density must be set up in the $s \to \infty$ limit.

https://doi.org/10.1017/9781009290227.011 Published online by Cambridge University Press

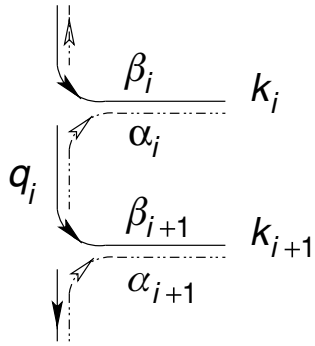

Fig. 10.1 Flow of longitudinal momenta in multiperipheral kinematics.

Recall that in perturbation theory transverse momenta were restricted by the virtual exchange propagators q_i in Fig. 10.1,

$$m^2 - q_i^2 = m^2 + \mathbf{q}_{i\perp}^2 + \alpha_q\beta_q s = m^2 + \mathbf{q}_{i\perp}^2 + \Big(\sum_{j\le i}\alpha_j\Big)\Big(\sum_{k\ge i+1}\beta_k\Big)s. \tag{10.6}$$

In the *perturbative* multiperipheral kinematics (9.27) all αs and βs were strongly ordered. The longitudinal part of the virtuality,

$$\alpha_q\beta_q s \simeq \big(\alpha_i + \cdots\big)\big(\beta_{i+1} + \cdots\big)s \simeq m_{i+1,\perp}^2 \cdot \frac{\beta_{i+1}}{\beta_i} \sim m^2 \cdot \frac{\beta_{i+1}}{\beta_i}, \tag{10.7}$$

was then negligible, and it was for m^2 to set the upper bound for the variation of $\mathbf{q}_{i\perp}^2$ in (10.6). If we increase $\bar{g}^2$, the 'comb' gets denser and denser, and at $\bar{g}^2 \sim 1$ we eventually reach the situation when the neighbouring βs become comparable, $\beta_i \ge \beta_{i+1}$. They are still ordered, but not *strongly ordered* anymore, which makes the longitudinal virtuality (10.7) comparable with m^2. This situation corresponds to $\langle s_{i,i+1}\rangle \gtrsim m^2$, that is to a unit density in rapidity.

Imagine now that with the increase of s the particle density keeps growing as $dn/d\eta = D(s)$. Having $D(s)$ particles with comparable Sudakov components inside a unit rapidity interval, (10.6) will be modified as follows:

$$m^2 - q_i^2 \simeq \mathbf{q}_{i\perp}^2 + m^2 + \big(D(s)\tilde{\alpha}\big)\big(D(s)\tilde{\beta}\big)s, \quad \tilde{\alpha}\tilde{\beta}s \sim m^2. \tag{10.8}$$

As a result, the transverse momentum integrals will spread much broader, up to $\mathbf{q}_{i\perp}^2 \lesssim D^2(s)m^2$, and produce the average $\mathbf{k}_\perp^2$ increasing with energy together with the density $D(s)$.

https://doi.org/10.1017/9781009290227.011 Published online by Cambridge University Press

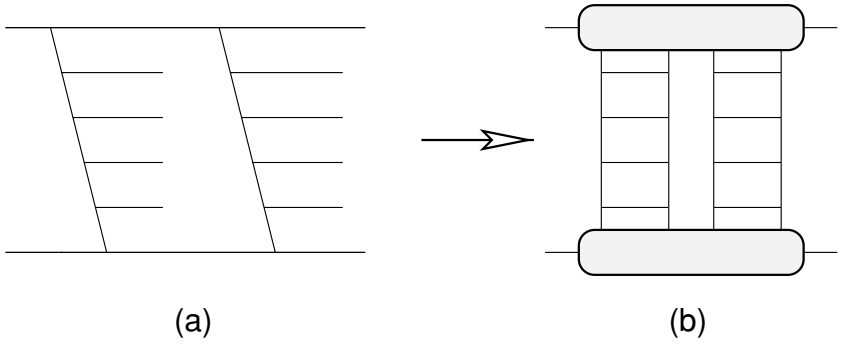

Fig. 10.2 Amplitude (a) and cross section (b) of the double-ladder process.

10.1.3 Large multiplicities and overlapping ladders

This does not mean, however, that in a collision of two hadrons there will be no events with multiplicities significantly larger than the average $\bar{n} \propto \ln s$. Even in the perturbative framework there is a simple way to obtain a large particle density, not breaking the restrictedness of $\langle \mathbf{k}_\perp^2 \rangle$. Let us draw a picture with two multiperipheral combs exchanged between the target and projectile. Squaring the diagram of Fig. 10.2(a) we will apply the previous analysis to the two ladders in Fig. 10.2(b) and will obtain the final-state multiplicity $\sim 2\bar{n}$, and therefore the double density in rapidity, while preserving limited transverse momenta inside each ladder.

When the interaction is strong, there is no reason for such a diagram to be any smaller than one ladder. There is, however, something bizarre about this picture.

Momentum distributions of particles in the two combs overlap perfectly. Why will they not interact, especially since the interaction is, once again, strong? On the other hand, if they *do* re-interact and become inseparable from the t-channel point of view, then our previous arguments will work linking the particle density to the average $\mathbf{k}_\perp^2$.

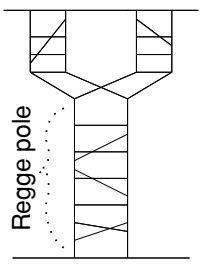

Actually, it is the t-channel we have to appeal to for the explanation. As we know, the Regge pole is a *bound state* in the t-channel.

But this implies that all the particles that 'propagate' in the t-channel must have *bounds* to each other; there cannot be two non-interacting groups of objects as in Fig. 10.2. In other words, such pictures do not belong to the *pole*.

The diagrams like that of Fig. 10.2 have a full right to exist but, if we believe in the pole approximation, they would better be small corrections

https://doi.org/10.1017/9781009290227.011 Published online by Cambridge University Press

describing density fluctuations on top of the underlying uniform plateau due to the Regge pole exchange.

10.1.4 Mueller–Kancheli diagram for inclusive spectrum

Let us calculate the inclusive spectrum corresponding to the Regge pole without appealing to the perturbation theory.

But first we make a qualitative remark to appreciate the key rôle played by the *factorization* feature of the Regge pole.

No matter how complicated the underlying diagrams are, due to the unitarity condition we have to take the imaginary part of the forward amplitude and extract one particle with a given momentum k in the intermediate multi-particle state,

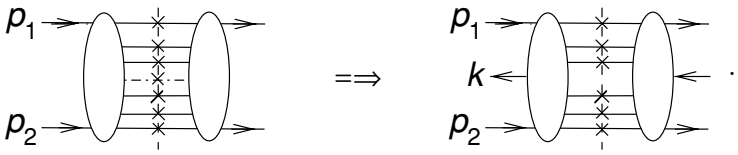

(10.9)

What distinguishes the upper part of the full block from the scattering amplitude of particles p_1 and k is that it is connected with the lower part by some particle lines. If the number of these lines increased with the total energy s, the average transverse momentum would also grow. Besides, if somewhere inside the process the number of exchanges depends on the initial energy, how can there be factorization on the l.h.s. of (10.9) which, as we have supposed, *is* described by the Regge pole?

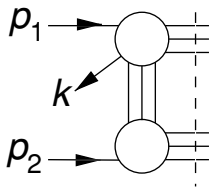

Repeating the same argument we isolate the particle k as shown in the l.h.s. of (10.10),

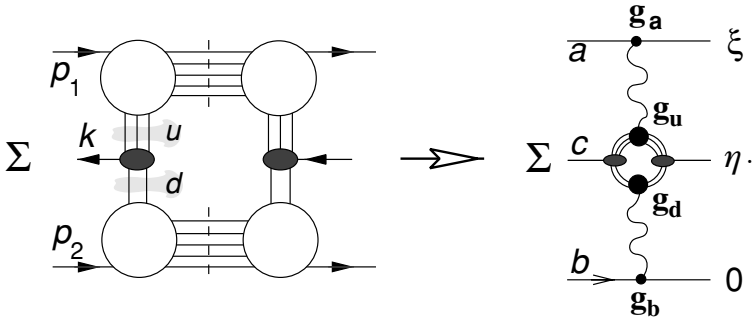

(10.10)

https://doi.org/10.1017/9781009290227.011 Published online by Cambridge University Press

It is connected to the top and bottom parts of the graph in a non-trivial manner via some particle 'bunches' u and d. If we additionally suppose that the interaction between particles is *local* in the rapidity space, then the central block $g^2_{c;u,d}$ that links the triggered particle (of type c) to the states u and d will span a finite rapidity interval of the order of unity.

Under these circumstances the invariant energies of the top and bottom blocks are large and we can substitute (imaginary parts of) the Regge pole amplitudes as shown on the r.h.s. of (10.10),

$$\sim \sum_{u,d} \cdot \left[g^r_a \, \mathrm{e}^{\alpha(0)(\xi-\eta)} g^r_u\right] \cdot g^2_{c;u,d} \cdot \left[g^r_d \, \mathrm{e}^{\alpha(0)\eta} g^r_b\right].$$

Since, due to factorization, the central part of the diagram does not depend on the total energy, we get the energy-independent rapidity plateau in the inclusive spectrum,

$$f(\mathbf{k}_\perp, \eta; s) = g^r_a g^r_b s^{\alpha(0)-1} \cdot \phi(\mathbf{k}_\perp); \quad \phi_c(\mathbf{k}_\perp) = \sum_{u,d} g^r_u \cdot g^2_{c;u,d} \cdot g^r_d \,. \tag{10.11}$$

The answer is represented by the Mueller–Kancheli reggeon diagram (Gribov, 2003),

$$f(\mathbf{k}_\perp, \eta; s) = \frac{1}{s} \cdot$$

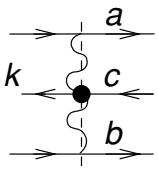

$$= \sigma^{ab}_{\mathrm{tot}} \cdot \phi_c(\mathbf{k}_\perp) \,. \tag{10.12}$$

To derive rigorously this important non-perturbative result, one considers the $3 \to 3$ scattering amplitude and continues it to complex angular momenta. If one supposes that there are Regge poles in $2 \to 2$ scattering at large s, then the asymptotic behaviour of $3 \to 3$ amplitude in the $s_1, s_2 \to \infty$, $s_1 s_2/s = \mathrm{const}$ limit is determined by the exchange of two Regge poles i, j,

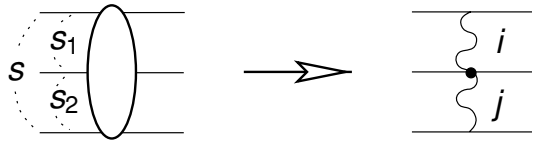

By taking the amplitude in which both i and j have vacuum quantum numbers, one arrives at (10.12).

10.1.5 Scaling in the fragmentation regions

The independence of the inclusive particle yield of the rapidity holds, obviously, if we take a particle far enough from the ends of the full rapidity

https://doi.org/10.1017/9781009290227.011 Published online by Cambridge University Press

interval, $\xi_\pm$. Only then the invariant energies between the triggered particle and the incoming ones are large, and we can substitute the reggeons for the corresponding scattering blocks.

What happens at the ends?

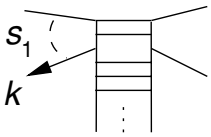

Let us take a particle with large rapidity, from the first ladder rungs on the side of the projectile. In this case we will be able to replace only the bottom part of the graph by a reggeon that covers a large rapidity interval $\eta - \xi_- = \eta$ (in the rest frame of the target p_2):

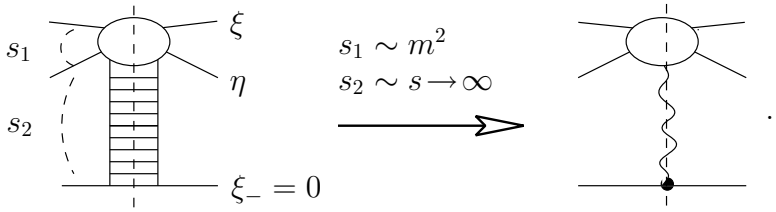

At the same time, there remains a serious dependence of the inclusive particle yield on the 'distance' $\xi - \eta$,

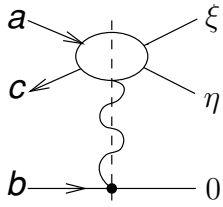

$$= \mathrm{e}^{\alpha(0)\eta}\psi(\mathbf{k}_\perp, s_1) \;=\; s^{\alpha(0)} g_\mathrm{b}^r \cdot \phi_\mathrm{ac}(\mathbf{k}_\perp, \xi - \eta). \quad (10.13)$$

Only after stepping away from the incident particle by about 2 units in rapidity, the system 'forgets' about the quantum numbers of the 'initiator' of the cascade, and the universal plateau starts developing.

Thus the inclusive spectrum consists of three regions: in addition to the plateau, two so-called *fragmentation regions* appear as shown in Fig. 10.3. They are called 'target fragmentation' and 'projectile fragmentation'.

The name *fragmentation* carries a deep meaning. According to (10.13), the structure of the fragmentation region of the *projectile*, in the interval between η_p and ξ in Fig. 10.3, depends on the type of the projectile a and that of the triggered particle c. Moving towards the kinematical boundary, the inclusive particle distribution may either increase as shown by the solid line (as in the reaction $\pi^- p \to \pi^- + X$), or drop ($\pi^- p \to \pi^+ + X$; dashed). At the same time it stays independent of the total energy s and of the type of the target b (the lower reggeon vertex g_b^r factors out into $\sigma_{\mathrm{tot}}^{ab}$). The same is true for target fragmentation, $\eta < \eta_t$.

https://doi.org/10.1017/9781009290227.011 Published online by Cambridge University Press

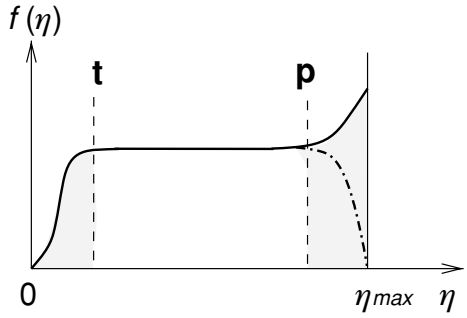

Fig. 10.3 Fragmentation regions and plateau in the inclusive spectum.

Since for fast particles

$$\mathrm{e}^{\xi-\eta} \simeq \frac{p_{1z}}{k_z} \equiv \frac{1}{x}, \quad \phi_{ac} = \phi_{ac}(\mathbf{k}_\perp, x),$$

the dependence on s_1 translates into the dependence on the *momentum fraction* x of the incident momentum p_1 that is carried by the triggered particle k.

This feature is called the *Feynman scaling* or the 'limiting fragmentation hypothesis'. In our picture it is a direct consequence of the reggeon factorization. With the increase of s the fragmentation regions in Fig. 10.3 just separate further while preserving their specific shapes.

It is clear that the scaling must manifest itself earlier in energy than the plateau since for the latter one needs both s_1 and s_2 to be sufficiently large. Indeed, the limiting fragmentation sets in already for s of the order of a few GeV and is well established experimentally. At the same time, a flat plateau appears only for $\xi \gtrsim 5$ corresponding to $s \simeq 150\,\mathrm{GeV}^2$.

What should one expect when comparing, e.g. the inclusive reactions

$$p\,p \;\to\; \pi^+ + X \quad \text{and} \quad p\,p \;\to\; \pi^- + X \;? \tag{10.14}$$

When we register a particle in the fragmentation region, we take it from the *residue* of the cut pomeron, and not much can be said about it. In particular, $\pi^\pm$ production is different not only in the fragmentation of the incident *pion* as we have just mentioned above, but also in the *proton* fragmentation region, since the proton feels very well the difference between π^+ and π^-.

However, in the plateau region quantum numbers of produced particles must be 'well equilibrated'. Here the particle is taken from inside the *vacuum pole* itself which is 'blind' to $\mathbf{I}_3$ or to (the sign of) the strangeness or the baryon charge. In this case the yields, e.g. of π^+ and π^- mesons must be identical. The symmetry between the reactions (10.14) holds

https://doi.org/10.1017/9781009290227.011 Published online by Cambridge University Press

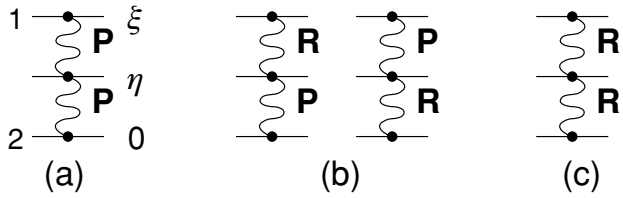

Fig. 10.4 Subleading corrections to the inclusive plateau density.

within a few percent. (One needs much higher energies to see protons and antiprotons 'equalize'.)*

Taking into consideration subleading reggeons **R** that also contribute to the forward scattering, such as $\boldsymbol{\rho}$ and $\mathbf{P}'$, one can study corrections to the asymptotics, as well as the transition between the plateau and fragmentation regions. Summing the diagrams of Fig. 10.4 gives for the particle density

$$\begin{aligned}\frac{f(\mathbf{k}_\perp,\eta;\xi)}{\sigma_{\rm tot}} &= \phi(\mathbf{k}_\perp) + c_1^R\phi'(\mathbf{k}_\perp)\mathrm{e}^{-\kappa(\xi-\eta)} \\ &\quad + c_2^R\phi'(\mathbf{k}_\perp)\mathrm{e}^{-\kappa\eta} + c_1^R c_2^R\phi''(\mathbf{k}_\perp)\mathrm{e}^{-\kappa\xi},\end{aligned} \tag{10.15}$$

where $\kappa = \alpha^P(0) - \alpha^R(0)$ is the shift between the pomeron intercept and that of the subleading reggeon R, and c_i are the reggeon residues normalized by the pomeron one, $c_i = g_i^R/g_i^P$. In reality, $\kappa \simeq \frac{1}{2}$ for the $\mathbf{f}(\mathbf{P}')$ and $\boldsymbol{\rho}$ trajectories, see Lecture 8. This shows that the graph Fig. 10.4(c) corresponding to the last term in (10.15) provides a 'flat', η-independent, pre-asymptotic correction $\propto 1/\sqrt{s}$ to the plateau height, while the magnitude of the corrections due to mixed graphs of Fig. 10.4(b) depends on rapidity. It increases towards the fragmentation region, introducing a *curvature* to the plateau–fragmentation transition.

Introducing an R pole into the two-particle inclusive cross section,

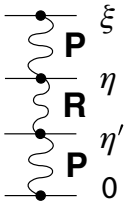

$$\propto \mathrm{e}^{-\kappa|\eta-\eta'|}, \tag{10.16}$$

* At nucleon–nucleon energies $s = 10^4$ GeV^2, the yield of antiprotons became practically equal to that of protons, as we learnt from experiments at the heavy ion collider RHIC, Brookhaven, NY, USA (ed.).

https://doi.org/10.1017/9781009290227.011 Published online by Cambridge University Press

results in a *positive* correlation ('attraction') between the particles since the non-leading reggeon tends to 'collapse', to reduce the difference of the rapidities.

In two different ways – by the extension of the perturbative analysis to the region $\bar{g}^2 \lesssim 1$ and by the analytic continuation of the six-point amplitude – under the assumption of the existence of the pomeron pole **P** in elastic scattering we arrive at the conclusion that multi-particle production processes at high energies have the following characteristic features.

(1) Final state hadrons are distributed homogeneously in η, away from the ends of the rapidity interval – the fragmentation regions,

$f(k_\perp, \eta; s) =$ 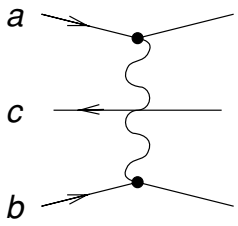

$= g_a g_b \, \phi_c(\mathbf{k}_\perp).$ (10.17a)

(2) In the fragmentation of the incident particle i, the spectrum depends only on the relative rapidity $f = f(\eta_i - \eta)$ – Feynman scaling,

$f(k_\perp, \eta; s) =$ 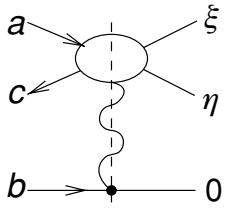

$= \phi_{ac}(\mathbf{k}_\perp, \xi - \eta) \, g_b.$ (10.17b)

(3) As a consequence, the average multiplicity increases logarithmically with collision energy,

$$\langle n \rangle \simeq \beta \ln \frac{s}{m^2} + \text{const}\,. \tag{10.17c}$$

Essentially, the key hypothesis that ensures the existence of the asymptotically constant rapidity plateau is that the transverse momenta in hadron interactions are limited.

https://doi.org/10.1017/9781009290227.011 Published online by Cambridge University Press

10.2 Inconsistency of the Regge pole approximation

Up to now we considered the Regge pole as the leading singularity in the complex angular momentum plane, assuming that all the other singularities of the partial amplitude are subleading poles, $s^{\alpha_{\mathbf{R}}}$, that give power-suppressed corrections and are irrelevant for the asymptotic behaviour.

We will show now that this assumption is contradictory.

10.2.1 Small-multiplicity events

Investigating perturbation theory, we have seen that the sum of ladder graphs had a Regge behaviour and, consequently, could provide a basis for the real Regge pole. Going beyond the perturbation theory, we have found that the qualitative features of typical inelastic processes with the production of $n \sim \bar{n}$ particles were similar to those of the multiperipheral ladder diagrams of the perturbative theory, although at $\bar{g}^2 \sim 1$.

What about small multiplicity events? As we know, in perturbation theory the topological cross sections σ_n follow the Poisson distribution

$$\sigma_{n+2} = \sigma_{\text{tot}} \cdot \mathrm{e}^{-\bar{n}} \frac{\bar{n}^n}{n!}, \tag{10.18}$$

and fall fast when one takes n away from the maximum, in particular on the left wing, $n \ll \bar{n}$.

Elastic-scattering contribution to σ_{tot}. Let us look at the elastic scattering – the first among small multiplicity processes – and calculate its contribution to the total cross section:

$$\sigma_2 = \frac{1}{16\pi} \int dq^2 \left| \frac{A_{\text{el}}(s, q^2)}{s} \right|^2 = \frac{1}{2s}$$

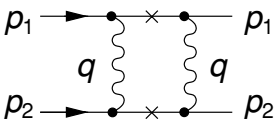

. (10.19)

Substituting the asymptotic elastic amplitude determined by the Pomeranchuk pole $\mathbf{P}$,

$$A_{\text{el}}(s, q^2) =$$

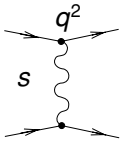

$$= g^2(t) \xi_{\alpha(q^2)} \left(\frac{s}{m^2} \right)^{\alpha(q^2)}, \quad \alpha(q^2) \simeq 1 + \alpha' q^2,$$

we derive

$$\sigma_2 \simeq \left(\frac{g^2(0)}{m^2} \right)^2 \cdot \frac{1}{32\pi\alpha'\xi}, \quad \xi = \ln \frac{s}{m^2}. \tag{10.20}$$

https://doi.org/10.1017/9781009290227.011 Published online by Cambridge University Press

Here we have used the fact that the momentum transfer in the integral is small since it is cut by the Regge radius, $|q^2| \simeq \mathbf{q}_\perp^2 \sim [\alpha' \ln(s/m^2)]^{-1}$, which allowed us to expand the pomeron trajectory, $\alpha(q^2) \simeq 1 + \alpha' q^2$, and to put $q^2 = 0$ in the reggeon vertex g and in the signature factor, $\xi \simeq i$.

We immediately see that the result we have just obtained is in a marked disagreement with the expectation based on the Poisson distribution (10.18) according to which the fraction of small multiplicity events is suppressed as a *power* of energy, $\sigma_2/\sigma_{\rm tot} \propto s^{-\beta_0}$, due to the logarithmic increase of the average $\bar{n} \simeq \beta_0 \ln s$. At the same time, (10.20) is suppressed at $s \to \infty$ only logarithmically.

10.2.2 Multiregge kinematics

This contradiction shows that the perturbative consideration fails when the number of final-state particles is small. It is clear what happened.

When the pair energy is small, two particles interact via the Born amplitude, 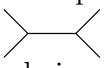 $= g^2/(m^2 - s_{12})$. (If we take the coupling $\bar{g}^2 \sim 1$, the exact amplitude is more complicated but not significantly different.) With the energy increasing, however, a new parameter appears, $\ln s$-enhanced terms become essential and the Born amplitude is replaced by the *reggeized amplitude* which corresponds to the 'floating spin' exchange in the t-channel. The standard $1/s$ amplitude gets enhanced:

$$s^{-1} \quad \Longrightarrow \quad s^{-1} \cdot s^{\beta(q^2)}.$$

When we treated final states with a number of particles of the order of the average multiplicity, typical pair energies,

$$\langle \ln s_{i,i+1} \rangle \simeq \frac{\ln s}{n} \sim \frac{\ln s}{\bar{n}} \sim (\bar{g}^2)^{-1},$$

were such that in the interaction between neighbours we could neglect the reggeization effects. In the elastic channel, on the contrary, we have a huge energy $s_{12} = s$ applied to two particles. In this situation we must modify the interaction amplitude by substituting the reggeon for the scalar particle exchange,

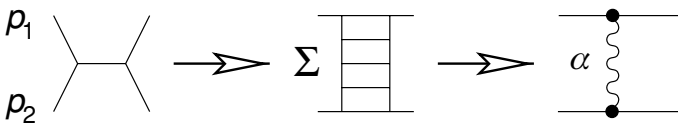

.

https://doi.org/10.1017/9781009290227.011 Published online by Cambridge University Press

Obviously, the same substitution must be done also when encountering a large pair energy *inside the multiperipheral ladder*. This happens when one has a wide *gap* in the rapidity distribution of the produced particles. By making the ladder more and more sparse, one can form many rapidity gaps, and ultimately arrive at the picture with all final particles (or compact groups of particles) widely separated in rapidity and connected by reggeons,

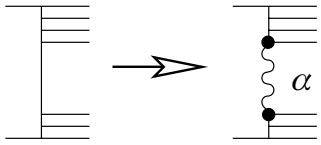

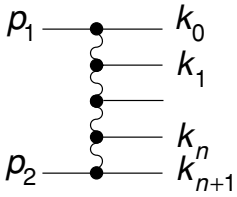

$$s_{i,i+1} \gg m^2, \quad s_{01}s_{12}\cdots s_{n,n+1} \sim sm^{2n}. \tag{10.21}$$

Such a situation is referred to as *multiregge kinematics* and corresponds to specific fluctuations in multi-particle production.

10.2.3 Multiregge amplitudes

We have to learn how various multiplicity fluctuations contribute to $\sigma_{\rm tot}$.

Derivation of the $2 \to 3$ *multiregge amplitude.* We start with three final-state particles. If an additional hadron is produced in the fragmentation region of one of the colliding particles, the pomeron exchange dominates (see Lecture 8) and we get a contribution of the order of σ_2,

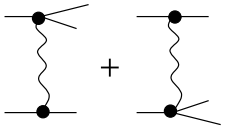

$$\delta\sigma_3 \sim \sigma_2.$$

Now we take the multiregge kinematics,

$$s_{12}, s_{23} \gg m^2, \quad s_{12}\cdot s_{23} \sim sm^2.$$

Omitting the complex phase, we can guess the answer straight away:

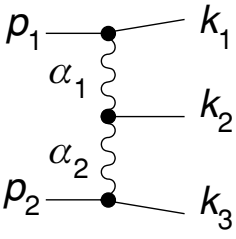

$$\sim g_1(\mathbf{k}_{1\perp})s_{12}^{\alpha(t_1)}\gamma(\mathbf{k}_{1\perp},\mathbf{k}_{3\perp})s_{23}^{\alpha(t_2)}g_2(\mathbf{k}_{3\perp}),$$
$$t_1 = (k_1 - p_1)^2, \quad t_2 = (k_3 - p_2)^2. \tag{10.22}$$

https://doi.org/10.1017/9781009290227.011 Published online by Cambridge University Press

It is not an easy task to derive rigorously the multiregge amplitudes by analytic continuation to complex j. The amplitude has specific analyticity in each of many sub-channels, and the *signature structure* of multi-point amplitudes becomes rather involved.

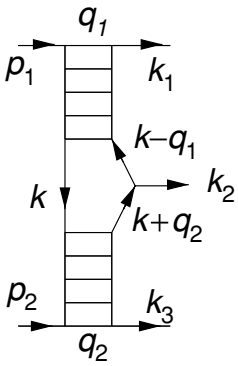

For our purpose of evaluating contributions to $\sigma_{\rm tot}$ in the s-channel, this subtlety is, however, irrelevant. So we can rely on the perturbative analogy and derive the $2 \to 3$ amplitude in the multiregge kinematics from the ladder picture. For the final particle momenta we write

$$\begin{aligned} k_1 &= \beta_1 p_+ + \frac{m_{1\perp}^2}{\beta_1} p_- + k_{1\perp}, \\ k_2 &= \beta_2 p_+ + \alpha_2 p_- + k_{2\perp}, \\ k_3 &= \frac{m_{3\perp}^2}{\alpha_3} p_+ + \alpha_3 p_- + k_{3\perp}. \end{aligned}$$

For momentum transfers q_i this gives

$$\begin{aligned} q_1 &\simeq (1-\beta_1)p_+ - \frac{\mathbf{k}_{1\perp}^2 + (1-\beta_1)m^2}{\beta_1 s} p_- - k_{1\perp}, \\ q_2 &\simeq (1-\alpha_3)p_- - \frac{\mathbf{k}_{3\perp}^2 + (1-\alpha_3)m^2}{\alpha_3 s} p_+ - k_{3\perp}. \end{aligned}$$

Then, due to the rapidity ordering and the momentum conservation,

$$\begin{aligned} \beta_3 \ll \beta_2 \ll \beta_1, \qquad & \beta_3 + \beta_2 + \beta_1 = 1; \\ \alpha_1 \ll \alpha_2 \ll \alpha_3, \qquad & \alpha_3 + \alpha_2 + \alpha_1 = 1, \end{aligned}$$

we have $(1-\beta_1) \simeq \beta_2$, $(1-\alpha_3) \simeq \alpha_2$, and the longitudinal components of the transferred momenta q_i become expressed in the multiregge kinematics via the observed particle momentum k_2:

$$\begin{aligned} q_1 &\simeq \beta_2 p_+ - \frac{\mathbf{k}_{1\perp}^2}{s} p_- - k_{1\perp}, \quad q_1^2 \simeq -\mathbf{k}_{1\perp}^2; \\ q_2 &\simeq \alpha_2 p_- - \frac{\mathbf{k}_{3\perp}^2}{s} p_+ - k_{3\perp}, \quad q_2^2 \simeq -\mathbf{k}_{3\perp}^2. \end{aligned}$$

We have to integrate over the loop momentum k,

$$k = \beta p_+ - \alpha p_- + k_\perp, \quad d^4k = \frac{s}{2}\, d\alpha\, d\beta\, d^2\mathbf{k}_\perp,$$

https://doi.org/10.1017/9781009290227.011 Published online by Cambridge University Press

whose Sudakov components determine the *invariant energies* of the top and bottom 'ladders',

$$\begin{aligned} s' &\equiv (p_1 - k)^2 = (\alpha+\gamma)(1-\beta)s + m^2 + k^2 \simeq \alpha s \equiv x \cdot s_{12}, \\ s'' &\equiv (p_2 + k)^2 = (1-\alpha)(\beta+\gamma)s + m^2 + k^2 \simeq \beta s \equiv y \cdot s_{23}. \end{aligned} \tag{10.23}$$

In (10.23) we have introduced momentum fractions

$$x = \alpha/\alpha_2, \qquad y = \beta/\beta_2, \tag{10.24}$$

and used $s_{12} = (k_1 + k_2)^2 \simeq \alpha_2 s$ and $s_{23} = (k_2 + k_3)^2 \simeq \beta_2 s$. Finally, let us have a look at the propagators:

$$\begin{aligned} m^2 - (k - q_1)^2 &= m^2 + (\mathbf{k} + \mathbf{k}_1)_\perp^2 + \alpha(\beta - \beta_2)s, \\ m^2 - k^2 &= m^2 + \mathbf{k}_\perp^2 + \alpha\beta s, \\ m^2 - (k + q_2)^2 &= m^2 + (\mathbf{k} - \mathbf{k}_3)_\perp^2 + (\alpha - \alpha_2)\beta s. \end{aligned} \tag{10.25}$$

The integrals over x and y converge at $x \sim y \sim 1$; therefore the invariant energies (10.23) are large and we can substitute Regge poles for the 'ladder' amplitudes,

$$\begin{aligned} A(s', q_1^2; k^2, (k - q_1)^2) &\sim g_a(q_1^2) \cdot \xi_{\alpha_1}(s')^{\alpha_1} \cdot \tilde{g}_1(q_1^2; k^2, (k - q_1)^2), \\ A(s'', q_2^2; k^2, (k + q_3)^2) &\sim g_b(q_2^2) \cdot \xi_{\alpha_2}(s'')^{\alpha_2} \cdot \tilde{g}_2(q_2^2; k^2, (k + q_2)^2). \end{aligned}$$

Here $\alpha_1 = \alpha_1(q_1^2)$ and $\alpha_2 = \alpha_2(q_2^2)$ are trajectories of the two reggeons, g_a, g_b are the standard reggeon–particle vertices, and the vertices $\tilde{g}$ contain the dependence on the virtualities of the participating particles. The answer has the form

$$\begin{aligned} A_{2\to 3}(s, \mathbf{k}_{1\perp}, \mathbf{k}_{2\perp}, \eta_2) &= g_1(q_1^2) g_2(q_2^2)\, \xi_{\alpha_1}\xi_{\alpha_2}\, m_{2\perp}^2 \cdot s_{12}^{\alpha_1} s_{23}^{\alpha_2} \times \gamma, \\ \gamma = \gamma(\mathbf{k}_{1\perp}, \mathbf{k}_{2\perp}) &= \int \frac{d^2\mathbf{k}_\perp}{2(2\pi)^2} \int \frac{dx\, dy}{(2\pi)^2 i} \frac{x^{\alpha_1} y^{\alpha_2}}{(1)(2)(3)} \tilde{g}_1\, \tilde{g}_2; \end{aligned} \tag{10.26a}$$

the propagators (10.25) in terms of the rescaled variables (10.24) read

$$\begin{aligned} (1) &= m^2 + (\mathbf{k} + \mathbf{k}_1)_\perp^2 + x(y-1) \cdot m_{2\perp}^2 - i\varepsilon, \\ (2) &= m^2 + \mathbf{k}_\perp^2 + x\, y \cdot m_{2\perp}^2 - i\varepsilon, \\ (3) &= m^2 + (\mathbf{k} - \mathbf{k}_3)_\perp^2 + (x-1)y \cdot m_{2\perp}^2 - i\varepsilon. \end{aligned} \tag{10.26b}$$

The concrete form of the function γ depends on details of the interaction. Importantly, it is a function of the transverse momenta and is independent of the energy invariants. Therefore we can look upon γ as a new reggeon–reggeon–particle vertex.

https://doi.org/10.1017/9781009290227.011 Published online by Cambridge University Press

Multiregge amplitudes $2 \to 2+n$. The generalization of (10.26) to the case of many particles separated by large rapidity gaps is straightforward. For the amplitude $A_{2\to 2+n}$ in the multi-regge kinematics (10.21) we can write (modulo the complex phase factor)

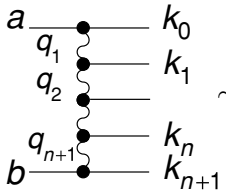

$$\sim g_a(q_1^2) s_{01}^{\alpha_1} \gamma_{12} s_{12}^{\alpha_2} \cdots \gamma_{n,n+1} s_{n,n+1}^{\alpha_{n+1}} g_b(q_{n+1}^2), \tag{10.27}$$

where each subscript in the trajectory α_i and the vertex $\gamma_{i,i+1}$ marks the dependence on the corresponding transferred transverse momentum, $\alpha_i = \alpha(-\mathbf{q}_{i\perp}^2)$, and $\gamma_{i,i+1} = \gamma(\mathbf{q}_{i\perp}, \mathbf{q}_{i+1\perp})$.

Contribution to σ_3 from the multiregge kinematics. Let us estimate the $2 \to 3$ cross section in the kinematical region (10.23). To begin with, the three-particle phase space volume is

$$\begin{aligned} d\Gamma_3 &= \frac{d^4k_1}{(2\pi)^4}\frac{d^4k_3}{(2\pi)^4}\prod_{i=1}^{3}\left[2\pi\delta_+(m^2-k_i^2)\right] \\ &= \frac{d\beta_1}{\beta_1}\frac{d\alpha_3}{\alpha_3}\frac{d^2\mathbf{k}_{1\perp}}{2(2\pi)^3}\frac{d^2\mathbf{k}_{3\perp}}{2(2\pi)^3}2\pi\delta_+(m^2+\mathbf{k}_{2\perp}^2-\alpha_2\beta_2 s) \\ &\simeq \frac{d\eta}{s}\frac{d^2\mathbf{k}_{1\perp}\,d^2\mathbf{k}_{3\perp}}{4(2\pi)^5}; \qquad d\eta = \frac{d\beta_2}{\beta_2}. \end{aligned} \tag{10.28}$$

Integrating the multiregge amplitude squared (10.26),

$$\sigma_3 = \frac{1}{J}\int d\Gamma_3 |A_{2\to 3}|^2,$$

and omitting the constant normalization factor, we have

$$\begin{aligned} \sigma_3 &\sim s^{2(\alpha(0)-1)}\int d\eta \int d\mathbf{k}_{1\perp}^2\, \mathrm{e}^{-2\alpha'(\xi-\eta)\mathbf{k}_{1\perp}^2}\int d\mathbf{k}_{3\perp}^2\, \mathrm{e}^{-2\alpha'\eta\,\mathbf{k}_{3\perp}^2} \\ &\sim \int_{\eta_0}^{\xi-\eta_0}\frac{d\eta}{\eta\,(\xi-\eta)} \sim \frac{\ln\xi}{\xi} \simeq \frac{\ln\ln s}{\ln s}; \qquad 1 \lesssim \eta_0 \ll \xi. \end{aligned} \tag{10.29}$$

Although this estimate is valid only in an academic limit $\xi \gg 1$, it demonstrates that, at least formally, σ_3 is enhanced as compared to the elastic contribution σ_2. The origin of this slight enhancement is a broad integration over rapidity of the particle k_2 from the plateau region.

https://doi.org/10.1017/9781009290227.011 Published online by Cambridge University Press

10.2.4 Multiplicity fluctuations and s-channel unitarity

The study of small multiplicities, $n \ll \bar{n}$, is a test of the Pomeranchuk pole hypothesis. If multiplicity fluctuations are weak and the pomeron is 'resistant' to the s-channel unitarity, we have a self-consistence theory at our disposal. If, however, fluctuations are strong and contribute 'too much' to σ_{tot}, then we have either to abandon altogether the initial idea that the pole is the rightmost singularity in the j plane, or to review the concept of $\mathbf{P}$ being an *isolated* singularity.

So, having started from the vacuum pole which from the s-channel point of view corresponds to an uniform particle distribution in rapidity,

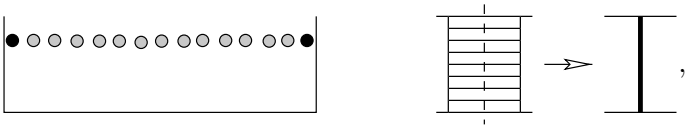

(10.30a)

we are driven by the unitarity relation in the s-channel to accept the existence of the processes that are difficult to accommodate into the pure Regge pole model. Thus, fluctuations in multi-particle production with large gaps in rapidity have led us to *reggeize* the amplitude by sending a reggeon between the two neighbouring particles with a large pair energy,

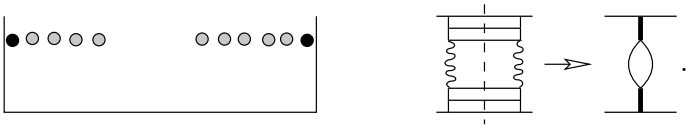

(10.30b)

This resulted in the cross section graphs containing the two poles which *coexist*, from the t-channel viewpoint. (Thick lines mark a cut-through $\mathbf{P}$.)

By broadening the gap we eventually arrive at the elastic scattering

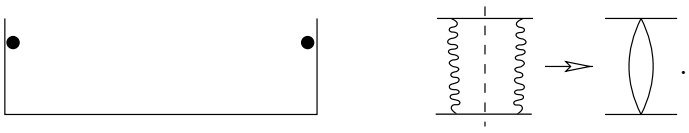

(10.30c)

As we have seen above, small multiplicity fluctuations contribute significantly to σ_{tot}; their contributions are suppressed only *logarithmically* in s, while we would expect a *power* smallness if there were only poles in the complex angular momentum plane.

The graphs with two 'parallel' reggeons, (10.30b) and (10.30c), make one think of *branch-cut singularities*, by an analogy with threshold branch cuts for usual particles. Another argument in favour of reggeon loops comes from the 'opposite side' – high multiplicity fluctuations. Indeed, we can imagine two multiperipheral cascades which will give rise to doubled

https://doi.org/10.1017/9781009290227.011 Published online by Cambridge University Press

plateau density,

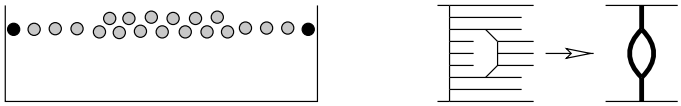

(10.30d)

In the cross section this corresponds again to a picture like (10.30b) but this time with all the pomerons being *cut*, $\mathbf{P} \to 2\,\mathrm{Im}\,\mathbf{P}$.

You may often hear people saying that the picture of multiple hadron production is very similar to statistics of a fluctuating gas. Literally, this analogy is wrong. The probability of finding in a gas just two molecules is exponentially small; in our case it *cannot* be small due to the optical theorem! It is the special rôle of elastic scattering that forces us to separate quasi-diffractive (fragmentation) processes from multi-particle production with $n \sim \bar{n}$. It is the latter for which the gas analogy works.

There are certain fluctuations that signal a catastrophic instability of our system. Let us discuss one particular very important fluctuation,

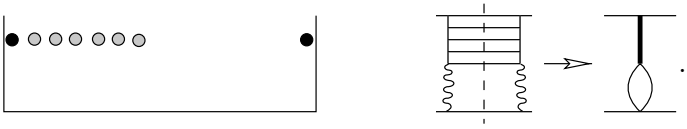

(10.30e)

10.2.5 Inelastic diffraction: triple-pomeron limit

This is the process in which one of the colliding particles scatters elastically, while the second one breaks up into a many-particle state. It may be referred to as the high-mass *inelastic diffraction*.

The reason for calling this process 'important' is, in the first place, its experimental accessibility.

It is not simple to investigate hadron collision events with rapidity gaps experimentally. One has to measure many particles (or rather their absence) to make sure that the event contains indeed rapidity gap(s). The process (10.30e) offers a much simpler option. Indeed, it is sufficient to register the leading scattered particle with sufficiently large energy, close to the initial one. Then the energy conservation law will ensure that there are no other energetic particles in the event, and we will get a gap in rapidity. Thus this process is a particular case of inclusive measurement with triggering of the particle from the very top, close to the kinematical boundary.

https://doi.org/10.1017/9781009290227.011 Published online by Cambridge University Press

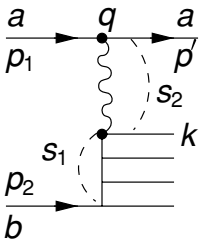

Let us look into kinematics. We choose for clarity the laboratory frame of the target, $\mathbf{p}_2 = \mathbf{0}$. Then

$$\begin{aligned} s &= (p_1 + p_2)^2 \simeq 2mp_{10} \gg m^2, \\ s_1 &= (q + p_2)^2 \simeq 2p_2 q = 2mq_0 \gg m^2. \end{aligned} \tag{10.31}$$

The invariant mass of the diffractive hadron system, $M^2 = s_1$, is determined by the energy transferred from the projectile to excite the target,

$$s_1 = \frac{q_0}{p_{10}}\, s \equiv (1 - x)s, \tag{10.32a}$$

where $x = p_0'/p_{10}$ is the energy fraction preserved by the scattered particle a. Practically the whole energy q_0 transferred to the target fragmentation block by the reggeon is carried by the fastest particle, the one on the top of the 'ladder', $k_0 \simeq q_0$. This allows us to evaluate the invariant energy s_2 corresponding to the size of the gap:

$$s_2 = (p' + k)^2 \simeq 2(p'k) \simeq p_0 \cdot \frac{m^2 + \mathbf{k}_\perp^2}{k_0} \simeq m_\perp^2 \frac{p_0}{q_0} = \frac{m_\perp^2}{1 - x}. \tag{10.32b}$$

By choosing x in the interval

$$\frac{m^2}{s} \ll 1 - x \ll 1 \tag{10.33}$$

we have the multiregge kinematics with s_1 and s_2 being both large, and

$$q^2 = -\frac{\mathbf{p}'^2_\perp}{x} - \frac{m^2(1-x)^2}{x} \simeq -\mathbf{p}'^2_\perp.$$

We square the amplitude and, replacing the target fragmentation block summed over all possible hadron states by $2\,\mathrm{Im}\,\mathbf{P}$, arrive at the graph shown in Fig. 10.5. This is called the *triple-reggeon limit*, or $3\mathbf{P}$ since all three reggeons are pomerons in our case.

Substituting the pomeron trajectory, $\alpha_{\mathbf{P}}(q^2) = 1 + \alpha' q^2$, and integrating over q^2 and x we get the probability of these fluctuations *increasing* with the energy:

$$\frac{\sigma_{3\mathbf{P}}}{\sigma_{\mathrm{tot}}} \propto \ln\ln\frac{s}{m^2}. \tag{10.34}$$

We arrive at a contradiction: we supposed that σ_{tot} is asymptotically constant, and found a *part* of it that grows infinitely.

https://doi.org/10.1017/9781009290227.011 Published online by Cambridge University Press

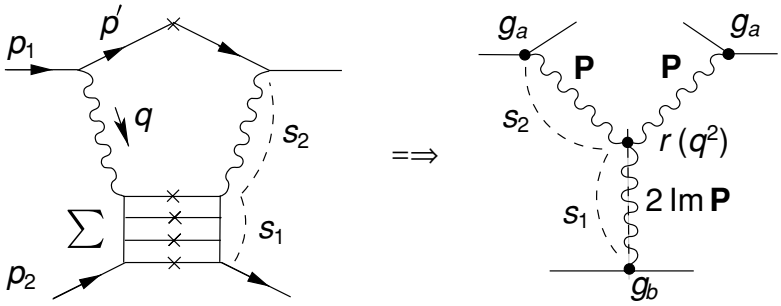

Fig. 10.5 Triple-regge limit for high-mass inelastic diffraction.

Let us calculate the contribution of the diagram of Fig. 10.5 to the total cross section. We have

$$\sigma_{3\mathbf{P}} = \frac{1}{J}\int \frac{d^3\mathbf{p}'}{2p_0'(2\pi)^3} g_a^2(q^2) s_2^{2\alpha(q^2)} r(q^2) 2 s_1^{\alpha(0)} g_b(0), \quad J = 2s, \tag{10.35a}$$

where g_a, g_b are couplings of $\mathbf{P}$ to the incoming particles 'a' and 'b', and r is a new three-reggeon vertex function. We did not write the signature factors $|\xi_\alpha|^2$, because at small q^2 which dominate the integral, $\xi_{\mathbf{P}} = i + \cot\frac{1}{2}\pi\alpha(q^2) \simeq i$.

Invoking (10.32) we absorb the factor $m_\perp^2$ from (10.32b) into redefining the vertex r to write

$$\begin{aligned}
\sigma_{3\mathbf{P}} &= \frac{g_b(0) s^{\alpha(0)-1}}{16\pi^2}\int\frac{dx}{x}\int\frac{d^2\mathbf{q}_\perp}{\pi} g_a^2(q^2)\cdot r(q^2)\cdot(1-x)^{\alpha(0)-2\alpha(q^2)} \\
&\simeq \frac{\sigma_{\rm tot}}{16\pi^2\, g_a(0)}\int\frac{dx}{1-x}\int d\mathbf{q}_\perp^2 (1-x)^{2\alpha'\mathbf{q}_\perp^2} g_a^2(q^2)\cdot r(q^2) \\
&= \frac{\sigma_{\rm tot}}{32\pi^2}\frac{g_a(0)}{\alpha'}\cdot r(0)\int\frac{dy}{y}, \qquad y = \ln\frac{1}{1-x}.
\end{aligned} \tag{10.35b}$$

Here we have extracted from under the integral the values of vertices g_a and r at $q^2 = -\mathbf{q}_\perp^2 = 0$, since the essential transverse momenta are small, due to the shrinkage of the diffractive cone, $\langle \mathbf{q}_\perp^2 \rangle \sim (\alpha' y)^{-1} \ll m^2$, at large y values. The integration over x in the multi-regge region (10.33) gives the catastrophic result announced above in (10.34):

$$\frac{\sigma_{3\mathbf{P}}}{\sigma_{\rm tot}} = r(0)\cdot\frac{g_a(0)}{32\pi^2\alpha'}\cdot\ln\ln\frac{s}{m^2}, \qquad \ln\frac{s}{m^2} \gg 1. \tag{10.36}$$

How can the apparent contradiction, $\sigma_{3\mathbf{P}} > \sigma_{\rm tot}$ in the $s \to \infty$ limit be handled? Let us examine the region of x in which the dangerous

https://doi.org/10.1017/9781009290227.011 Published online by Cambridge University Press

contribution has been accumulated. Actual integration limits are

$$s_1 = (1-x)s > \Lambda m^2 \gg m^2, \quad s_2 \sim \frac{m^2}{1-x} > \Lambda m^2 \gg m^2,$$

where Λ is a large number. First of all, in order to apply the reggeon amplitudes to both the top and the bottom parts of the diagram, we need to take at least $\Lambda \gtrsim 10$ which corresponds to stepping by about 2 units in rapidity from the projectile and the target (we know that only then the *plateau* starts emerging). So, we have to 'renormalize' the argument of the logarithm; conservatively,

$$\ln\frac{s}{m^2} \quad \Longrightarrow \quad \ln\frac{s}{100\,m^2}.$$

Secondly, when we evaluated the integral over $\mathbf{q}_\perp$ we have ignored the size proper of the proton, embedded in $g_a(q^2)$. Hence, another modification:

$$\ln\ln s \quad \Longrightarrow \quad \ln\left(\frac{R^2}{\alpha'} + \ln s\right), \qquad \frac{R^2}{\alpha'_{\mathbf{P}}} \sim 4.$$

Moreover, the factor before $\ln\ln$ in (10.36) is numerically small. At present energies, the inelastic diffraction constitutes less than 10% of $\sigma_{\rm tot}$. And $\ln\ln$ is hardly a function: it is indistinguishable from a constant. A real contradiction may appear only at fantastically high energies; in fact we have only $\ln\ln s = 5$ when s equals the mass squared of the Universe!

However, in order to accept this as an excuse we need to have a theory in which the mass of the Universe enters and solves this $\ln\ln$ phenomenon, which option is likely to belong to the domain of science fiction.

Therefore we must view this apparent contradiction as a serious fault of the theory we are constructing.

Fortunately, there is a more practical way to resolve the problem. In the three-reggeon diagram we have, in fact, introduced a new notion, that of the *reggeon interaction vertex* $r(q^2)$. We have supposed that the value $r(0)$ is finite. Further, we shall see that the vanishing of reggeon interaction vertices at $\mathbf{q}_\perp = 0$ in one of the possible solutions of the problem of taming multiplicity fluctuations.

In Lecture 15 we will return to the multiplicity fluctuation pattern and will discuss physical reasons for inelastic processes to *vanish* in the forward direction, $\mathbf{q}_\perp = 0$.

10.2.6 Multiparticle production with large rapidity gaps

High-mass inelastic diffraction is not the only multiplicity fluctuation going wild. Another example, due to K. Ter-Martirosyan, builds up on the multi-regge amplitudes (10.27) that describe the production of many

https://doi.org/10.1017/9781009290227.011 Published online by Cambridge University Press

particles with large rapidity gaps between them.

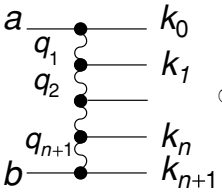

$$\propto g_a s_{01}^{\alpha_1} \gamma_{12} s_{12}^{\alpha_2} \cdots \gamma_{n,n+1} s_{n,n+1}^{\alpha_{n+1}} g_b.$$

The cross section $\sigma_{2\to 2+n}$ can be calculated in the same way as for ordinary multiperipheral ladders. There is one essential difference: the Regge-dependence of the ladder cell amplitude on the pair energy has to be taken into account

$$M_i \sim \xi_{\alpha_i} s_{i-1,i}^{\alpha(q_i^2)} \sim s_{i-1,i}^{\alpha(0)} \mathrm{e}^{-\alpha' \mathbf{q}_{i\perp}^2 y_i}; \quad y_i = \ln \frac{s_{i-1,i}}{m^2},\ i = 1, \ldots, n+1. \tag{10.37}$$

Here y_i is the relative rapidity of two particles $i-1$ and i, which we will treat as large, $y_i \gg 1$. The cross section contains $n+1$ integrals over transverse momenta $\mathbf{q}_i$, $i = 1, \ldots, n+1$. These integrals are cut from above by Regge radii at sufficiently high energies $s_{i,i+1}$:

$$\mathbf{q}_{i\perp}^2 \lesssim \frac{1}{\alpha' \ln s_{i,i+1}} = \frac{1}{\alpha' y} \ll m^2, \tag{10.38}$$

therefore we put $\mathbf{q}_{i\perp} = 0$ in the vertices, g and $\gamma_{i,i+1}$, as we have done before in a number of occasions. Squaring the matrix element (10.37) and integrating over $\mathbf{q}_i$, we get the product of inverse relative rapidities. We are left with n integrations over ordered rapidities of final state particles k_i, $i = 1, \ldots, n$, which we represent as $n+1$ independent integrals over rapidity *differences*, y_i, satisfying the kinematical relation (10.21):

$$\frac{\delta\sigma_n}{\sigma_{\mathrm{tot}}} \sim \frac{\gamma^n(0,0)}{(2\alpha')^{n+1}} \int_{\ln\Lambda}^{\xi} \frac{dy_1\, dy_2 \cdots dy_{n+1}}{y_1 y_2 \cdots y_{n+1}}\, \delta\left(\sum_{i=1}^{n+1} y_i - \xi\right). \tag{10.39}$$

Here we have combined the product $\prod s_{i-1,i}^{\alpha(0)} = s^{\alpha(0)}$ and the vertices $g_{a,b}(0)$ into the total cross section and put $\ln\Lambda$ for the lower limits of rapidity integrals to justify the usage of the multi-reggeon approximation (see the discussion above). As far as the formal $s \to \infty$ asymptote is concerned, the leading contribution comes from the configurations when one of variables is much larger than the rest, $y_{(k)} \simeq \xi \gg y_i$, $i \neq k$, and we derive the answer for the fraction of the cross section due to the production

https://doi.org/10.1017/9781009290227.011 Published online by Cambridge University Press

of a sparse n-particle final state in the multi-regge kinematics:

$$\frac{\delta\sigma_n}{\sigma_{\rm tot}} \simeq \text{const} \cdot (n+1)\frac{(\ln\xi)^n}{\xi}. \tag{10.40a}$$

(Importantly, there is no $n!$ in the denominator.) Our derivation implied

$$\ln\langle y_i\rangle \simeq \ln\frac{\xi}{n} \simeq \ln\frac{\bar{n}}{n} \gg \frac{R^2}{\alpha'} \simeq 4,$$

so we better 'soften' our result (10.40a) as follows,

$$\frac{\delta\sigma_n}{\sigma_{\rm tot}} \simeq \text{const} \cdot \frac{n+1}{\xi}\left(\ln\frac{\xi}{n}\right)^n. \tag{10.40b}$$

Still, the formal contradiction is there. Let us demonstrate that at $s \to \infty$ we can always find such a 'sparse ladder' the cross section of which grows arbitrarily large. Expressing n as a fraction of the mean multiplicity, $n \equiv \xi/F$, $\ln F \gg 1$, and keeping F fixed, we obtain

$$\frac{\delta\sigma_{\beta\langle n\rangle}}{\sigma_{\rm tot}} \sim \frac{\text{const}}{F}(\ln F)^{\xi/F} \propto s^{(\ln\ln F)/F},$$

that is, the fraction of events increasing as a (very small but finite) *power* of energy! Again, we arrive at a contradiction with the pomeron pole hypothesis: multiplicity fluctuations tend to ruin it (unless in (10.39) the pomeron–pomeron interaction vertex vanishes in the origin, $\gamma(0,0) = 0$).

10.3 Reggeon branch cuts and their rôle

What is the composition of the total cross section in our modified picture?

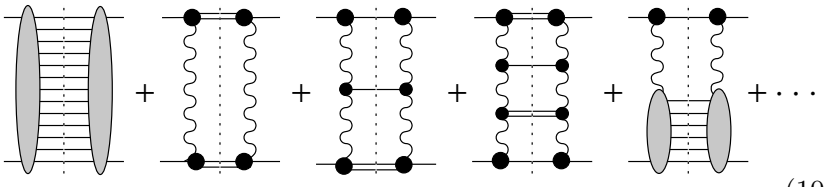

(10.41)

In addition to the multiperipheral 'ladders' with $n \sim \bar{n}(s)$, we have the contribution of the (quasi)elastic scattering, as well as a series of terms describing multiparticle production with large rapidity gaps between (groups of) hadrons.

We have introduced the pomeron pole as the *rightmost singularity* in the vacuum channel. This implied that the total cross section was

https://doi.org/10.1017/9781009290227.011 Published online by Cambridge University Press

asymptotically given, with *power accuracy*, by the imaginary part of the pomeron amplitude,

$$\sigma_{\rm tot} \to \operatorname{Im} A^{\mathbf{P}}(s,0) = \frac{1}{2}$$ 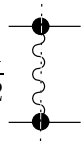 $$\times \left(1 + \mathcal{O}\left(\frac{1}{s^a}\right)\right), \quad s \to \infty. \tag{10.42a}$$

From the perturbation theory we learned that the 's-channel content' of the pomeron pole corresponds to the first term of (10.41),

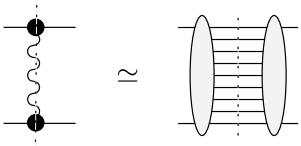

$$\simeq \quad . \tag{10.42b}$$

Where in (10.42a) are then the *logarithmically behaving* 'fluctuation' terms that are present in (10.41)? To add an insult to injury, according to the logic that we have advocated before, the Regge pole must accommodate the structures that are *dynamically bound* in the t-channel; but the just-mentioned missing terms hardly satisfy this criterion, especially the first – elastic – one. There are two possible escapes:

(1) $\sigma_{\rm tot}$ in (10.41) differs from the multiperipheral model (10.42b) by a sum of positive terms. If we were to rescue the pure Regge pole approximation, we could imagine that the prescription (10.42b) was simply inaccurate, and in fact

$$A^{\mathbf{P}}_{\rm exact} = A^{\mathbf{P}}_{\rm ladder} - \Delta,$$

with Δ a *small correction* compensating the unwanted contributions in the optical theorem (10.41).

(2) An alternative possibility is that we made a mistake not in identifying the pomeron pole with the characteristic rapidity plateau as in (10.42b) but in the very assumption that the pole is the only significant contributor to the full amplitude, even in the $s \to \infty$ limit:

$$A_{\rm exact} = A^{\mathbf{P}} - \Delta; \quad \frac{\Delta}{A^{\mathbf{P}}} \sim \frac{1}{\ln s}.$$

The second option – the only viable one, as it turns out – implies that the pomeron *is not* the leading singularity; more accurately, is not an *isolated* leading singularity. To legalize the existence of the corrections to $\operatorname{Im}\mathbf{P}$ that are suppressed only *logarithmically* in s in the unitarity condition,

https://doi.org/10.1017/9781009290227.011 Published online by Cambridge University Press

there must exist other singularities in the j-plane, weaker than the pole, positioned at the same point $j = 1$ at $t = 0$.

10.3.1 Enter reggeon branchings

Two-pomeron correction to the elastic amplitude. Let us examine the first correction to the elastic scattering amplitude due to s-channel iteration of the pomeron exchange:

2 Im 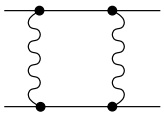 = 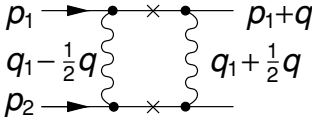

$$= \int \frac{d^4 q_1}{(2\pi)^4} g^2(t_1) g^2(t_2) \xi_{\alpha(t_1)} s^{\alpha(t_1)} \cdot \xi^*_{\alpha(t_2)} s^{\alpha(t_2)} \cdot 2\pi\delta((p_1 - q_1)^2 - m^2) 2\pi\delta((p_2 + q_1)^2 - m^2), \tag{10.43}$$

where

$$t_1 \simeq -(\mathbf{q}_1 - \tfrac{1}{2}\mathbf{q})^2_\perp, \;\; t_2 \simeq -(\mathbf{q}_1 + \tfrac{1}{2}\mathbf{q})^2_\perp.$$

A simple calculation yields

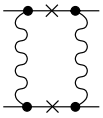

$$\simeq s^{2\alpha(t/4)-1} g^4 |\xi_\alpha|^2 \int \frac{d^2\mathbf{q}_{1\perp}}{2(2\pi)^2} \exp\{-2\alpha' \mathbf{q}^2_{1\perp} \cdot \ln s\} \tag{10.44}$$

$$\simeq g^4(t/4) \left|\xi_{\alpha(t/4)}\right|^2 \frac{s^{2\alpha(t/4)-1}}{16\pi\, \alpha' \ln s}\,.$$

Here we substituted $t_1 = t_2 = t/4$ in the pre-exponential factors since the transverse momentum integral at large $\xi = \ln s$ selects small $\mathbf{q}_{1\perp}$. Taking the forward scattering amplitude, $t \simeq -\mathbf{q}^2_\perp = 0$, we recover the correction σ_2 that we have calculated above in (10.20). The energy exponent of (10.44) corresponds to a new singularity whose trajectory is

$$j_2 = 2\alpha(t/4) - 1 \;\simeq\; 1 + \tfrac{1}{2}\alpha' t. \tag{10.45}$$

It has a twice-smaller slope than the pomeron; at $t = 0$ the position of this new singularity coincides with that of the pomeron. The pre-exponential factor $(\ln s)^{-1}$ in (10.44) shows that this is not a pole but a *branch cut* in the angular momentum plane.

Multi-reggeon moving branch point singularities. In the next lecture we will demonstrate that the necessity of branch cuts in the complex angular momentum plane follows directly from the t-channel. They are driven by

https://doi.org/10.1017/9781009290227.011 Published online by Cambridge University Press

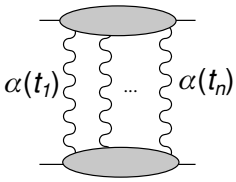

Regge poles. Once a Regge pole $\alpha(t)$ is introduced into the theory, it generates a series of moving branch-point singularities with trajectories

$$j_n(t) \;=\; n\,\alpha\left(\frac{t}{n^2}\right) - n + 1, \tag{10.46}$$

the expression generalizing (10.45) to all n and originating from the exchange of n reggeons in the t-channel.

Historical remark, and a lesson. The question of branch-point singularities (branchings) has a curious history. First, people thought that such angular momentum singularities cannot exist, which is the case in the non-relativistic quantum mechanics. Then it was understood that they must be present. Searching for a model for branching, a diagram of Fig. 10.6(a) was suggested based on the perturbative picture of a pole as a ladder.

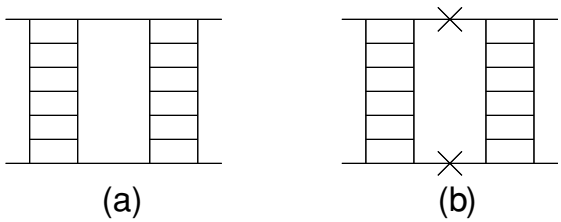

Fig. 10.6 The diagram (a) falls with s much faster than its imaginary part (b).

It was soon realized, however, that with s increasing this diagram is *falling fast*, as a power of s. This looks puzzling, since we have just seen above that its *imaginary part* shown in Fig. 10.6(b) is rather large and models the two-reggeon branching very well indeed!

The point is, the diagram (a) has *many cuts* in s, many 'imaginary parts', so to say, while we have selected in (b) one specific cut. In the full sum of all possible discontinuities of the diagram (a) different 'imaginary parts' cancel, making the picture with parallel ladders a wrong model for the branching. We will discuss this issue in detail in Lecture 12 where we will understand the physical reason behind this cancellation and construct the true s-channel image of the t-channel branch-point singularity.

But already at this stage there is an important message to take on board. When we have been discussing multiplicity fluctuations, we cut the diagrams for $\sigma_{\rm tot}$ in (10.41) 'in the middle', and avoided cutting through reggeons (where possible). At the same time, the reggeon amplitudes have

https://doi.org/10.1017/9781009290227.011 Published online by Cambridge University Press

a non-trivial complexity themselves. In the complete theory we must take these alternative discontinuities into full account. We had already a hint in this direction when we saw how different cuts of the same graph with a pomeron loop produced a rapidity-gap event, (10.30b), and a double multiplicity fluctuation, (10.30d).

10.3.2 Branchings in non-vacuum and vacuum channels

Let us look at the behaviour of (10.46) at large n and fixed t,

$$j_n(t) \simeq (n-1)(\alpha(0)-1)+\alpha(0), \quad n \to \infty.$$

There are three qualitatively different patterns.

$\alpha(0)<1$. High order branchings move to the left and become insignificant.

$\alpha(0)>1$. No-go: $j_n \to +\infty$ violates analyticity/causality: the corresponding $A(s)$ would grow faster than any power of energy.†

$\alpha(0)=1$. In this exceptional case branch cuts accumulate at $j=1$ and are all important. (From the consideration of s-channel phenomena, we already learnt that they have to be.)

The first case applies to all Regge trajectories but **P**.

A remarkable link between t-channel resonances and the asymptotic energy behaviour of corresponding scattering amplitudes in the s-channel stay intact after we take into account reggeon branchings.

For example, at large s the charge exchange reaction $\pi^- p \to \pi^0 n$ is dominated by the ρ Regge pole having trajectory $\beta(0) \simeq 0.5$. Repeating such a reggeon in the t channel produces a $1/\sqrt{s}$ suppressed correction:

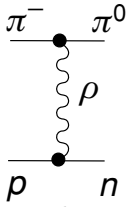

$$j_2(0)-j_1(0) = (2\beta(0)-1)-\beta(0) = -(1-\beta(0)) \simeq 0.5.$$

Another possibility is to send a pomeron in parallel to the ρ pole. In this case we get

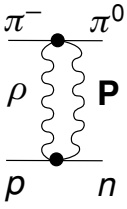

$$j_2(0) = \alpha(0)+\beta(0)-1 = \beta(0).$$

The power falloff of the amplitude remains the same. However, the scattering angle dependence at small $t<0$ will be affected by branching corrections.

† Dynamics of t-channel branch cuts *almost* contains the Froissart theorem!

https://doi.org/10.1017/9781009290227.011 Published online by Cambridge University Press

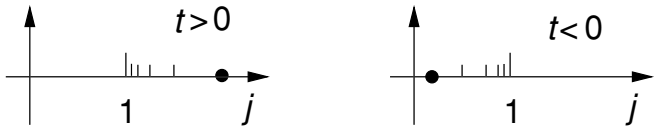

Fig. 10.7 Relative position of the pomeron pole and branchings in j-plane.

Return to the most interesting vacuum channel case, $\alpha(0) = 1$. Let us draw what happens in the j-plane (Fig. 10.7). If $t > 0$, branchings are on the left from the pole and accumulate at $j = 1$. In the physical region of the s-channel, $t < 0$, the picture looks dramatic: the pole is no longer the rightmost singularity. This means that pomeron branchings are likely to seriously modify the t-dependence of the scattering amplitude.

As for the total cross section, here a difficult story starts. Prior to addressing the problem we must develop adequate means first. To connect colliding particles by parallel reggeons as we did before is not enough. We need to learn how reggeons *interact* among themselves.

This is exactly what happens, from the t-channel point of view, in high-mass inelastic diffraction and multi-gap events, in particular, those very fluctuations that we found most damaging for self-consistency of the pomeron picture:

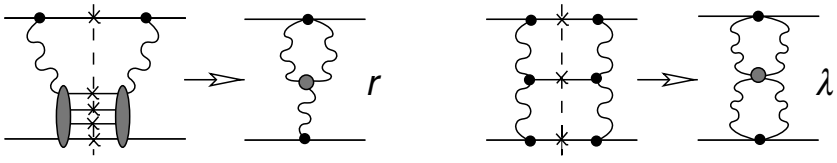

One possibility is that branchings are significant to such an extent that they turn out to play the *dominant* rôle, changing the energy behaviour of the cross section, of the plateau density, etc. (the so-called 'strong coupling' regime).

Another possible scenario preserves the asymptotic constancy of σ_{tot}. One can construct a self-consistent theory if all effective reggeon interaction vertices (r, λ, etc.) vanish when the transverse momenta flowing through participating reggeons tend to zero. In this ('weak coupling') solution pomeron branchings, and multiplicity fluctuations along with them, are kept under control as corrections. A recently found unexpected consequence of this theory runs as follows: if total cross sections are asymptotically constant, they must tend to *one and the same* constant for all scattering processes!

But first we have to return to the t-channel and to complex angular momenta.

https://doi.org/10.1017/9781009290227.011 Published online by Cambridge University Press